EUROPEAN ORGANIZATION FOR NUCLEAR RESEARCH

CERN-PH-EP/2004-055
November 1, 2004

Search for an Invisibly-Decaying Higgs Boson at LEP

arXiv:hep-ex/0501033v1 13 Jan 2005

L3 Collaboration

Abstract

A search for a Higgs boson produced in e^+e^- collisions in association with a Z boson and decaying into invisible particles is performed. Data collected at LEP with the L3 detector at centre-of-mass energies from 189 GeV to 209 GeV are used, corresponding to an integrated luminosity of 0.63 fb^{-1}. Events with hadrons, electrons or muons with visible masses compatible with a Z boson and missing energy and momentum are selected. They are consistent with the Standard Model expectations. A lower limit of 112.3 GeV is set at 95% confidence level on the mass of the invisibly-decaying Higgs boson in the hypothesis that its production cross section equals that of the Standard Model Higgs boson. Relaxing this hypothesis, upper limits on the production cross section are derived.

Submitted to *Phys. Lett. B*

1 Introduction

The Standard Model of the electroweak interactions [1] relies on the Higgs mechanism [2] to explain the observed masses of the elementary particles. A consequence of this mechanism is the existence of an additional particle, the Higgs boson. Direct searches at the LEP e^+e^- collider for the Standard Model Higgs boson, H, produced in the Higgs-strahlung process $e^+e^- \to HZ$ did not observe a significant excess of events over the Standard Model expectations [3–5]. These searches are based on the hypothesis that the Higgs boson mainly decays into b quarks. Searches in which this hypothesis is relaxed and the Higgs boson is allowed to decay into a generic hadronic final state also yield negative results [6]. In addition, no signs of the Higgs boson were found in cases in which anomalous couplings would affect its production and decay mechanisms [7].

However, a Higgs boson which decays into stable weakly-interacting particles would have escaped detection in all these searches. Such possibility has been extensively proposed in literature for the case of Higgs bosons decaying into the lightest supersymmetric particles [8], fourth-generation neutrinos [9], neutrinos in the context of theories with extra space dimensions [10], majorons [10, 11] or into a general scalar gauge singlet added to the Standard Model [12].

This Letter describes the search for an invisibly-decaying Higgs boson, h, produced through the Higgs-strahlung process $e^+e^- \to hZ$. Decays of the Z boson into hadrons, electron pairs and muon pairs are considered and analyses are devised to select events with hadrons or leptons and missing energy and momentum. Data collected by the L3 detector [13] at LEP at centre-of-mass energies $\sqrt{s} = 189 - 209$ GeV are analysed. They correspond to a total integrated luminosity of 0.63 fb^{-1}, as detailed in Table 1.

The results presented in this Letter supersede those of previous L3 studies [14, 15], as the complete high-luminosity and high-energy data sample is investigated and the previously published data collected at $\sqrt{s} = 189$ GeV [15] are re-analysed with improved procedures. Similar searches were also performed by other LEP collaborations [3, 16].

2 Event simulation

To optimise the selection criteria and determine the efficiency to detect a possible signal, samples of Higgs-boson events are generated using the PYTHIA Monte Carlo program [17] for masses of the Higgs boson, m_{h}, between 50 GeV and 120 GeV in steps between 5 GeV and 10 GeV.

The following Monte Carlo programs are used to model Standard Model processes: KK2f [18] for $e^+e^- \to q\bar{q}$, $e^+e^- \to \mu^+\mu^-$ and $e^+e^- \to \tau^+\tau^-$, BHWIDE [19] for Bhabha scattering, and PHOJET [20] and DIAG36 [21] for hadron and lepton production in two-photon collisions, respectively. Four-fermion final states relevant for the analysis of events with hadrons and missing energy are generated with PYTHIA for Z-boson pair-production and the $e^+e^- \to Ze^+e^-$ process and with KORALW [22] for W-boson pair-production, with the exception of the $e^+e^- \to We\nu \to qqe\nu$ process, modelled with EXCALIBUR [23]. All four-fermion processes with charged leptons and neutrinos in the final states, relevant for the analysis of events with leptons and missing energy, are generated with KandY [24].

For each centre-of-mass energy, the number of simulated background events corresponds to at least 50 times the number of expected events, up to a maximum of 7.5 million KandY events, except for two-photon interactions and Bhabha scattering for which twice and seven times the collected luminosity is simulated, respectively.

The L3 detector response is simulated using the GEANT program [25], which takes into

account the effects of energy loss, multiple scattering and showering in the detector. Time-dependent inefficiencies of the different subdetectors, as monitored during the data-taking period, are taken into account in the simulation procedure.

3 Selection of events with hadrons and missing energy

A preselection identifies events compatible with the production of a heavy invisible particle and a Z boson decaying into hadrons. High multiplicity events are retained if their visible energy, E_{vis}, satisfies $0.3 < E_{vis}/\sqrt{s} < 0.65$ and have a visible mass between 60 GeV and 115 GeV. No identified leptons or photons of energy above 10 GeV are allowed in these events. To suppress the large background from hadron production in two-photon collisions and events from the $e^+e^- \to q\bar{q}\gamma$ process with a high-energy and low polar-angle photon, the missing momentum of the event is required to point inside the detector: its polar angle with respect to the beam axis, θ_{miss}, must satisfy $|\cos\theta_{miss}| < 0.9$. In addition, the event is reconstructed into two jets by means of the DURHAM algorithm [26] and the angle between the jets is required to be smaller than 175°. Events with large energy deposits in the low-angle calorimeters are also rejected. After the preselection, 779 events are selected in data while 772 events are expected from Standard Model processes, as detailed in Table 2. The signal efficiencies depend on m_{h}, and vary from 52% up to 59%. Up to 90% of the background comes from four-fermion processes and 10% from fermion-pair production.

Two selections are devised in order to retain high efficiency for light and heavy Higgs bosons. The "light-Higgs selection" is applied to events where the relativistic velocity of the reconstructed hadron system, β, satisfies $\beta > 0.4$. The "heavy-Higgs selection" is applied to the remaining events.

The dominant background for the light-Higgs selection arises from W boson pair-production where one of the W bosons decays into hadrons and the other into leptons and from the $e^+e^- \to We\nu$ process. Two additional selection criteria are applied to reduce these backgrounds: $\zeta_{jet} < 100°$ and $\theta_3 < 330°$, where ζ_{jet} is the angle between the jets in the plane transverse to the beam direction and θ_3 is the sum of the three inter-jet angles defined if the event is reconstructed into a three-jet topology with the DURHAM algorithm. The last cut rejects genuine three-jet events from W-boson pair-production where a W boson decays into hadrons and the other into tau leptons which decay into hadrons. Figures 1a and 1b present the distributions of ζ_{jet} and θ_3.

The heavy-Higgs selection enforces the topology of a heavy undetected particle by means of two cuts against the background from pair production of either W bosons or fermions. The mass recoiling to the hadron system is required to be greater than 80 GeV and the energy deposited in the calorimeters in a 60° cone around the direction of the missing momentum is required to be smaller than 20 GeV. The distributions of these variables are shown in Figures 1c and 1d.

The results of the light- and heavy-Higgs selections are presented in Table 2, while Table 3 lists the signal efficiencies. In total, 475 events are selected in data and 474 are expected from Standard Model processes, dominated by four fermion final-states. Figures 2a–d present the distributions of the visible mass of the hadronic system and of the mass recoiling to the hadronic system, for the light- and heavy-Higgs selections. No indication for an excess of events in the signal regions is observed.

The sensitivity to a possible Higgs signal is enhanced by building a discriminating variable for each of the two analyses. This variable combines [27] information from the visible and recoil

masses, as well as the jet widths and the parameter y_{23} of the DURHAM algorithm for which three jets are reconstructed in a two-jet event. Figures 2e and 2f present the distributions of the discriminating variable for events selected by the light- and heavy-Higgs selections, respectively. A good agreement between the observations and the Standard Model predictions is observed.

4 Selection of events with leptons and missing energy

The selection of events possibly originating from an invisibly-decaying Higgs boson and a Z boson decaying into leptons proceeds from the L3 analysis of W boson pair-production where either both W bosons decay into an electron and a neutrino, or both decay into a muon and a neutrino [28]. Events with an electron or a muon pair are selected if the least and most energetic leptons have energies above 5 GeV and 25 GeV, respectively. The angle of the leptons with respect to the beam direction, θ, must satisfy $|\cos\theta| < 0.96$. In the case of electrons, to reduce the background from the forward-peaked Bhabha scattering, at least one of the electrons must satisfy $|\cos\theta| < 0.92$. To suppress background from fermion pair-production and cosmic rays, the angle between the two leptons in the plane transverse to the beam direction, ζ_ℓ, must satisfy $\zeta_\ell < 172^\circ$. Residual background from cosmic rays is rejected by requiring the leptons to have a signal in the scintillator time-of-flight counters compatible with the beam crossing. Finally, the presence of undetected particles is enforced by requiring the event momentum transverse to the beam direction, p_t, to be greater than 8 GeV.

A total of 147 electron pairs and 115 muon pairs are selected, in good agreement with the Standard Model expectation of 136 and 130 events, respectively. These events are mostly due to four-fermion production, as summarised in Table 4. Signal efficiencies depend on m_{h} and are about 60% and 50% for final states with electrons and muons, respectively. The distributions after this preselection of the visible and recoil masses of the lepton pairs, as well as of the visible energy of the events are shown in Figures 3. A good agreement between data and Monte Carlo expectations is found.

The main criteria to isolate signal events is to require the consistency of the visible mass with the mass of the Z boson. Two ranges are chosen, 86 GeV $-$ 95 GeV for electrons and 80 GeV $-$ 99 GeV for muons, as illustrated in Figures 3a and 3b. In addition, the event selection requires $|\cos\theta_{miss}| < 0.9$. In order to reduce the four-fermion background and increase the signal sensitivity, events are classified according to the value of the recoil mass. If it is below 85 GeV, a light-Higgs selection is further applied. A heavy-Higgs selection is applied otherwise. The light-Higgs selection relies on three cuts, common to both final states: $\zeta_\ell > 100^\circ$, $E_{vis}/\sqrt{s} < 0.57$ and $p_z/\sqrt{s} < 0.25$, where p_z is the projection of the event momentum along the direction of the beams. In addition, events with muons are required to satisfy $p_t > 14$ GeV. The heavy-Higgs selection requires $E_{vis}/\sqrt{s} < 0.45$ for both final states and $p_t > 20$ GeV for final states with muons.

After these cuts, a total of 6 events are observed in the electron final-state and 9 in the muon final state, consistent with the Standard Model background expectations of 9.7 and 11.1 events, respectively, largely due to four-fermion final states. These results are summarised in Table 4 while the signal efficiencies are detailed in Table 3. The distributions of the visible mass of the events, after all other cuts are applied, are shown in Figures 4a and 4b, while Figures 4c and 4d show the distributions of the recoil mass. No indication for a Higgs signal is found in these distributions.

5 Results

No evidence is found for a signal due to the production of invisibly-decaying Higgs bosons in association with a Z boson decaying into hadrons, electrons or muons either in the total counts of events or in the distributions of the discriminant variables and the recoil masses. The results of this search are therefore expressed in terms of limits on m_{h}. In the hypothesis that an invisibly-decaying Higgs boson is produced with the same cross section of the Standard Model Higgs boson, a technique based on a log-likelihood ratio [5] is used to calculate the confidence level $1 - \mathrm{CL_b}$ that the observed events are consistent with background expectation. The distributions of the final discriminating variables of the hadron selection, presented in Figures 2e and 2f, and of the recoil masses to the lepton system, presented in Figures 4c and 4d, are used in the calculation which yields the results presented in Figure 5 for the hadron and lepton analyses in terms of the log-likelihood ratio and $1 - \mathrm{CL_b}$ as a function of m_{h}. No structure which could hint to the presence of a signal is observed. The confidence level for the presence of the expected signal [5], $\mathrm{CL_s}$, is also depicted in Figure 5 for both analyses, as a function of m_{h}. Lower limits at 95% confidence level (CL) on m_{h} are derived from the results of the hadron and lepton analyses as 112.1 GeV and 91.3 GeV, respectively, in good agreement with the expected limits of 111.4 GeV and 88.4 GeV.

These limits include the systematic uncertainties on the signal efficiency and the background normalisation listed in Table 5. These follow from the limited Monte Carlo statistics and from the uncertainties on the cross sections of the background processes. Additional sources of systematic uncertainties, collectively indicated as "detector response" comprise uncertainties in the determination of the energy scale of the detector and possible discrepancies between data and Monte Carlo in the tails of the variables used in the event selection. The inclusion of the systematic uncertainties lowers the limits by about 200 MeV

The results of the combination of the hadron and lepton selections is expressed in terms of the log-likelihood ratio and $\mathrm{CL_s}$ as a function of m_{h} shown in Figures 6a and 6b. A lower limit to the mass of an invisibly-decaying Higgs boson is derived at 95% CL as:

$$m_{\mathrm{h}} > 112.3 \text{ GeV},$$

in good agreement with the expected limit of 111.6 GeV. This limit holds in the hypothesis that the invisibly-decaying Higgs boson is produced with the same cross section of the Standard Model Higgs boson. If this hypothesis is relaxed, upper limits as a function of m_{h} are extracted on the ratio of the invisibly-decaying Higgs-boson cross section to the Standard Model one, as shown in Figure 6c. These limits are translated into the upper limits on the cross section for the production of an invisibly-decaying Higgs boson as a function of m_{h} shown in Figure 6d.

References

[1] S.L. Glashow, Nucl. Phys. **22** (1961) 579; S. Weinberg, Phys. Rev. Lett. **19** (1967) 1264; A. Salam, *Elementary Particle Theory*, edited by N. Svartholm (Almqvist and Wiksell, Stockholm, 1968), p. 367.

[2] P.W. Higgs, Phys. Lett. **12** (1964) 132; P.W. Higgs, Phys. Rev. Lett. **13** (1964) 508; P.W. Higgs, Phys. Rev. **145** (1966) 1156; F. Englert and R. Brout, Phys. Rev. Lett. **13** (1964) 321; G.S.Guralnik, C.R. Hagen and T.W.B. Kibble, Phys. Rev. Lett. **13** (1964) 585.

[3] ALEPH Collab., A. Heister *et al.*, Phys. Lett. **B 526** (2002) 191;

[4] DELPHI Collab., J. Abdallah *et al.*, Eur. Phys. J. **C 32** (2004) 145; L3 Collab. P. Achard *et al.*, Phys. Lett. **B 517** (2001) 319; OPAL Collab., G. Abbiendi *et al.*, Eur. Phys. J. **C 26** (2003) 479.

[5] ALEPH, DELPHI, L3 and OPAL Collab., The LEP Working Group for Higgs Boson Searches, Phys. Lett. **B 565** (2003) 61.

[6] ALEPH Collab. H. Heister *et al.*, Phys. Lett. **B 544** (2002) 25; L3 Collab. P. Achard *et al.*, Phys. Lett. **B 583** (2004) 14; OPAL Collab. G. Abbiendi *et al.*, Phys. Lett. **B 597** (2004) 11.

[7] L3 Collab. P. Achard *et al.*, Phys. Lett. **B 589** (2004) 89.

[8] A. Djouadi *et al.* Phys. Lett. **B 376** (1996) 220. K. Griest and H.E. Haber, Phys. Rev. **D 37** (1998) 719;

[9] K. Belotsky *et al.* Phys. Rev. **D 68** (2003) 054027.

[10] S.P. Martin and J.D. Wells, Phys. Rev. **D 60** (1999) 035006.

[11] F. de Campos *et al.* Phys. Rev. **D 55** (1997) 1316, and references therein.

[12] T. Binoth and J.J. van der Bij, Z. Phys. **C 75** (1997) 17.

[13] L3 Collab., B. Adeva *et al.*, Nucl. Instr. Meth. **A 289** (1990) 35; L3 Collab., O. Adriani *et al.*, Phys. Rep. **236** (1993) 1; J.A. Bakken *et al.*, Nucl. Instr. Meth. **A 275** (1989) 81; O. Adriani *et al.*, Nucl. Instr. Meth. **A 302** (1991) 53; B. Adeva *et al.*, Nucl. Instr. Meth. **A 323** (1992) 109; K. Deiters *et al.*, Nucl. Instr. Meth. **A 323** (1992) 162; M. Chemarin *et al.*, Nucl. Instr. Meth. **A 349** (1994) 345; M. Acciarri *et al.*, Nucl. Instr. Meth. **A 351** (1994) 300; G. Basti *et al.*, Nucl. Instr. Meth. **A 374** (1996) 293; A. Adam *et al.*, Nucl. Instr. Meth. **A 383** (1996) 342.

[14] L3 Collab., M. Acciarri *et al.*, Phys. Lett. **B 418** (1997) 389.

[15] L3 Collab., M. Acciarri *et al.*, Phys. Lett. **B 485** (2000) 85.

[16] DELPHI Collab., J. Abdallah *et al.*, Eur. Phys. Jour **C 32** (2004) 475; OPAL Collab., G. Abbiendi *et al.*, Eur. Phys. J. **C 7** (1999) 407.

[17] PYTHIA versions 5.722 and 6.1 are used; T. Sjöstrand, preprint CERN-TH/7112/93 (1993), revised 1995; T. Sjöstrand, Comp. Phys. Comm. **82** (1994) 74; T. Sjöstrand, preprint hep-ph/0001032 (2000).

[18] KK2f version 4.13 is used; S. Jadach, B.F.L. Ward and Z. Wąs, Comp. Phys.Comm. **130** (2000) 260.

[19] BHWIDE version 1.03 is used; S. Jadach, W. Placzek and B.F.L. Ward, Phys. Lett. **B 390** (1997) 298.

[20] PHOJET version 1.05 is used; R. Engel, Z. Phys. **C 66** (1995) 203; R. Engel and J. Ranft, Phys. Rev. **D 54** (1996) 4244.

[21] DIAG36 Monte Carlo; F.A. Berends, P.H. Daverfeldt, R. Kleiss, Nucl. Phys. **B 253** (1985) 441.

[22] KORALW version 1.33 is used; M. Skrzypek *et al.*, Comp. Phys. Comm. **94** (1996) 216; M. Skrzypek *et al.*, Phys. Lett. **B 372** (1996) 289.

[23] EXCALIBUR version 1.11 is used; F.A. Berends, R. Kleiss and R. Pittau, Comp. Phys. Comm. **85** (1995) 437.

[24] KandY runs concurrently KORALW version 1.51 and YFSWW3 version 1.16; S. Jadach *et al.*, Comp. Phys. Comm. **119** (1999) 272; S. Jadach *et al.*, Phys. Rev. **D 65** (2002) 090310; S. Jadach *et al.*, Comp. Phys. Comm. **140** (2001) 475.

[25] GEANT version 3.15 is used; R. Brun *et al.*, preprint CERN DD/EE/84-1 (1985), revised 1987. The GHEISHA program (H. Fesefeldt, RWTH Aachen Report PITHA 85/02, 1985) is used to simulate hadronic interactions.

[26] S. Catani *et al.*, Phys. Lett. **B 269** (1991) 432; S. Bethke *et al.*, Nucl. Phys. **B 370** (1992) 310.

[27] L3 Collab., P. Achard *et al.* Phys. Lett. **B 545** (2002) 30.

[28] L3 Collab., P. Achard *et al.* Phys. Lett. **B 600** (2004) 22.

The L3 Collaboration:

P.Achard,[20] O.Adriani,[17] M.Aguilar-Benitez,[25] J.Alcaraz,[25] G.Alemanni,[23] J.Allaby,[18] A.Aloisio,[29] M.G.Alviggi,[29] H.Anderhub,[49] V.P.Andreev,[6,34] F.Anselmo,[8] A.Arefiev,[28] T.Azemoon,[3] T.Aziz,[9] P.Bagnaia,[39] A.Bajo,[25] G.Baksay,[26] L.Baksay,[26] S.V.Baldew,[2] S.Banerjee,[9] Sw.Banerjee,[4] A.Barczyk,[49,47] R.Barillère,[18] P.Bartalini,[23] M.Basile,[8] N.Batalova,[46] R.Battiston,[33] A.Bay,[23] F.Becattini,[17] U.Becker,[13] F.Behner,[49] L.Bellucci,[17] R.Berbeco,[3] J.Berdugo,[25] P.Berges,[13] B.Bertucci,[33] B.L.Betev,[49] M.Biasini,[33] M.Biglietti,[29] A.Biland,[49] J.J.Blaising,[4] S.C.Blyth,[35] G.J.Bobbink,[2] A.Böhm,[1] L.Boldizsar,[12] B.Borgia,[39] S.Bottai,[17] D.Bourilkov,[49] M.Bourquin,[20] S.Braccini,[20] J.G.Branson,[41] F.Brochu,[4] J.D.Burger,[13] W.J.Burger,[33] X.D.Cai,[13] M.Capell,[13] G.Cara Romeo,[8] G.Carlino,[29] A.Cartacci,[17] J.Casaus,[25] F.Cavallari,[39] N.Cavallo,[36] C.Cecchi,[33] M.Cerrada,[25] M.Chamizo,[20] Y.H.Chang,[44] M.Chemarin,[24] A.Chen,[44] G.Chen,[7] G.M.Chen,[7] H.F.Chen,[22] H.S.Chen,[7] G.Chiefari,[29] L.Cifarelli,[40] F.Cindolo,[8] I.Clare,[13] R.Clare,[38] G.Coignet,[4] N.Colino,[25] S.Costantini,[39] B.de la Cruz,[25] S.Cucciarelli,[33] R.de Asmundis,[29] P.Déglon,[20] J.Debreczeni,[12] A.Degré,[4] K.Dehmelt,[26] K.Deiters,[47] D.della Volpe,[29] E.Delmeire,[20] P.Denes,[37] F.DeNotaristefani,[39] A.De Salvo,[49] M.Diemoz,[39] M.Dierckxsens,[2] C.Dionisi,[39] M.Dittmar,[49] A.Doria,[29] M.T.Dova,[10,♯] D.Duchesneau,[4] M.Duda,[1] B.Echenard,[20] A.Eline,[18] A.El Hage,[1] H.El Mamouni,[24] A.Engler,[35] F.J.Eppling,[13] P.Extermann,[20] M.A.Falagan,[25] S.Falciano,[39] A.Favara,[32] J.Fay,[24] O.Fedin,[34] M.Felcini,[49] T.Ferguson,[35] H.Fesefeldt,[1] E.Fiandrini,[33] J.H.Field,[20] F.Filthaut,[31] P.H.Fisher,[13] W.Fisher,[37] I.Fisk,[41] G.Forconi,[13] K.Freudenreich,[49] C.Furetta,[27] Yu.Galaktionov,[28,13] S.N.Ganguli,[9] P.Garcia-Abia,[25] M.Gataullin,[32] S.Gentile,[39] S.Giagu,[39] Z.F.Gong,[22] G.Grenier,[24] O.Grimm,[49] M.W.Gruenewald,[16] M.Guida,[40] V.K.Gupta,[37] A.Gurtu,[9] L.J.Gutay,[46] D.Haas,[5] D.Hatzifotiadou,[8] T.Hebbeker,[1] A.Hervé,[18] J.Hirschfelder,[35] H.Hofer,[49] M.Hohlmann,[26] G.Holzner,[49] S.R.Hou,[44] B.N.Jin,[7] P.Jindal,[14] L.W.Jones,[3] P.de Jong,[2] I.Josa-Mutuberría,[25] M.Kaur,[14] M.N.Kienzle-Focacci,[20] J.K.Kim,[43] J.Kirkby,[18] W.Kittel,[31] A.Klimentov,[13,28] A.C.König,[31] M.Kopal,[46] V.Koutsenko,[13,28] M.Kräber,[49] R.W.Kraemer,[35] A.Krüger,[48] A.Kunin,[13] P.Ladron de Guevara,[25] I.Laktineh,[24] G.Landi,[17] M.Lebeau,[18] A.Lebedev,[13] P.Lebrun,[24] P.Lecomte,[49] P.Lecoq,[18] P.Le Coultre,[49] J.M.Le Goff,[18] R.Leiste,[48] M.Levtchenko,[27] P.Levtchenko,[34] C.Li,[22] S.Likhoded,[48] C.H.Lin,[44] W.T.Lin,[44] F.L.Linde,[2] L.Lista,[29] Z.A.Liu,[7] W.Lohmann,[48] E.Longo,[39] Y.S.Lu,[7] C.Luci,[39] L.Luminari,[39] W.Lustermann,[49] W.G.Ma,[22] L.Malgeri,[18] A.Malinin,[28] C.Maña,[25] J.Mans,[37] J.P.Martin,[24] F.Marzano,[39] K.Mazumdar,[9] R.R.McNeil,[6] S.Mele,[18,29] L.Merola,[29] M.Meschini,[17] W.J.Metzger,[31] A.Mihul,[11] H.Milcent,[18] G.Mirabelli,[39] J.Mnich,[1] G.B.Mohanty,[9] G.S.Muanza,[24] A.J.M.Muijs,[2] B.Musicar,[41] M.Musy,[39] S.Nagy,[15] S.Natale,[20] M.Napolitano,[29] F.Nessi-Tedaldi,[49] H.Newman,[32] A.Nisati,[39] T.Novak,[31] H.Nowak,[48] R.Ofierzynski,[49] G.Organtini,[39] I.Pal,[46] C.Palomares,[25] P.Paolucci,[29] R.Paramatti,[39] G.Passaleva,[17] S.Patricelli,[29] T.Paul,[10] M.Pauluzzi,[33] C.Paus,[13] F.Pauss,[49] M.Pedace,[39] S.Pensotti,[27] D.Perret-Gallix,[4] D.Piccolo,[29] F.Pierella,[8] M.Pioppi,[33] P.A.Piroué,[37] E.Pistolesi,[27] V.Plyaskin,[28] M.Pohl,[20] V.Pojidaev,[17] J.Pothier,[18] D.Prokofiev,[34] J.Quartieri,[40] G.Rahal-Callot,[49] M.A.Rahaman,[9] P.Raics,[15] N.Raja,[9] R.Ramelli,[49] P.G.Rancoita,[27] R.Ranieri,[17] A.Raspereza,[48] P.Razis,[30] D.Ren,[49] M.Rescigno,[39] S.Reucroft,[10] S.Riemann,[48] K.Riles,[3] B.P.Roe,[3] L.Romero,[25] A.Rosca,[48] C.Rosemann,[1] C.Rosenbleck,[1] S.Rosier-Lees,[4] S.Roth,[1] J.A.Rubio,[18] G.Ruggiero,[17] H.Rykaczewski,[49] A.Sakharov,[49] S.Saremi,[6] S.Sarkar,[39] J.Salicio,[18] E.Sanchez,[25] C.Schäfer,[18] V.Schegelsky,[34] H.Schopper,[21] D.J.Schotanus,[31] C.Sciacca,[29] L.Servoli,[33] S.Shevchenko,[32] N.Shivarov,[42] V.Shoutko,[13] E.Shumilov,[28] A.Shvorob,[32] D.Son,[43] C.Souga,[24] P.Spillantini,[17] M.Steuer,[13] D.P.Stickland,[37] B.Stoyanov,[42] A.Straessner,[20] K.Sudhakar,[9] G.Sultanov,[42] L.Z.Sun,[22] S.Sushkov,[1] H.Suter,[49] J.D.Swain,[10] Z.Szillasi,[26,¶] X.W.Tang,[7] P.Tarjan,[15] L.Tauscher,[5] L.Taylor,[10] B.Tellili,[24] D.Teyssier,[24] C.Timmermans,[31] Samuel C.C.Ting,[13] S.M.Ting,[13] S.C.Tonwar,[9] J.Tóth,[12] C.Tully,[37] K.L.Tung,[7] J.Ulbricht,[49] E.Valente,[39] R.T.Van de Walle,[31] R.Vasquez,[46] V.Veszpremi,[26] G.Vesztergombi,[12] I.Vetlitsky,[28] D.Vicinanza,[40] G.Viertel,[49] S.Villa,[38] M.Vivargent,[4] S.Vlachos,[5] I.Vodopianov,[26] H.Vogel,[35] H.Vogt,[48] I.Vorobiev,[35,28] A.A.Vorobyov,[34] M.Wadhwa,[5] Q.Wang,[31] X.L.Wang,[22] Z.M.Wang,[22] M.Weber,[18] S.Wynhoff,[37] L.Xia,[32] Z.Z.Xu,[22] J.Yamamoto,[3] B.Z.Yang,[22] C.G.Yang,[7] H.J.Yang,[3] M.Yang,[7] S.C.Yeh,[45] An.Zalite,[34] Yu.Zalite,[34] Z.P.Zhang,[22] J.Zhao,[22] G.Y.Zhu,[7] R.Y.Zhu,[32] H.L.Zhuang,[7] A.Zichichi,[8,18,19] B.Zimmermann,[49] M.Zöller.[1]

1 III. Physikalisches Institut, RWTH, D-52056 Aachen, Germany§
2 National Institute for High Energy Physics, NIKHEF, and University of Amsterdam, NL-1009 DB Amsterdam, The Netherlands
3 University of Michigan, Ann Arbor, MI 48109, USA
4 Laboratoire d'Annecy-le-Vieux de Physique des Particules, LAPP,IN2P3-CNRS, BP 110, F-74941 Annecy-le-Vieux CEDEX, France
5 Institute of Physics, University of Basel, CH-4056 Basel, Switzerland
6 Louisiana State University, Baton Rouge, LA 70803, USA
7 Institute of High Energy Physics, IHEP, 100039 Beijing, China△
8 University of Bologna and INFN-Sezione di Bologna, I-40126 Bologna, Italy
9 Tata Institute of Fundamental Research, Mumbai (Bombay) 400 005, India
10 Northeastern University, Boston, MA 02115, USA
11 Institute of Atomic Physics and University of Bucharest, R-76900 Bucharest, Romania
12 Central Research Institute for Physics of the Hungarian Academy of Sciences, H-1525 Budapest 114, Hungary‡
13 Massachusetts Institute of Technology, Cambridge, MA 02139, USA
14 Panjab University, Chandigarh 160 014, India
15 KLTE-ATOMKI, H-4010 Debrecen, Hungary¶
16 Department of Experimental Physics, University College Dublin, Belfield, Dublin 4, Ireland
17 INFN Sezione di Firenze and University of Florence, I-50125 Florence, Italy
18 European Laboratory for Particle Physics, CERN, CH-1211 Geneva 23, Switzerland
19 World Laboratory, FBLJA Project, CH-1211 Geneva 23, Switzerland
20 University of Geneva, CH-1211 Geneva 4, Switzerland
21 University of Hamburg, D-22761 Hamburg, Germany
22 Chinese University of Science and Technology, USTC, Hefei, Anhui 230 029, China△
23 University of Lausanne, CH-1015 Lausanne, Switzerland
24 Institut de Physique Nucléaire de Lyon, IN2P3-CNRS,Université Claude Bernard, F-69622 Villeurbanne, France
25 Centro de Investigaciones Energéticas, Medioambientales y Tecnológicas, CIEMAT, E-28040 Madrid, Spain♭
26 Florida Institute of Technology, Melbourne, FL 32901, USA
27 INFN-Sezione di Milano, I-20133 Milan, Italy
28 Institute of Theoretical and Experimental Physics, ITEP, Moscow, Russia
29 INFN-Sezione di Napoli and University of Naples, I-80125 Naples, Italy
30 Department of Physics, University of Cyprus, Nicosia, Cyprus
31 Radboud University and NIKHEF, NL-6525 ED Nijmegen, The Netherlands
32 California Institute of Technology, Pasadena, CA 91125, USA
33 INFN-Sezione di Perugia and Università Degli Studi di Perugia, I-06100 Perugia, Italy
34 Nuclear Physics Institute, St. Petersburg, Russia
35 Carnegie Mellon University, Pittsburgh, PA 15213, USA
36 INFN-Sezione di Napoli and University of Potenza, I-85100 Potenza, Italy
37 Princeton University, Princeton, NJ 08544, USA
38 University of Californa, Riverside, CA 92521, USA
39 INFN-Sezione di Roma and University of Rome, "La Sapienza", I-00185 Rome, Italy
40 University and INFN, Salerno, I-84100 Salerno, Italy
41 University of California, San Diego, CA 92093, USA
42 Bulgarian Academy of Sciences, Central Lab. of Mechatronics and Instrumentation, BU-1113 Sofia, Bulgaria
43 The Center for High Energy Physics, Kyungpook National University, 702-701 Taegu, Republic of Korea
44 National Central University, Chung-Li, Taiwan, China
45 Department of Physics, National Tsing Hua University, Taiwan, China
46 Purdue University, West Lafayette, IN 47907, USA
47 Paul Scherrer Institut, PSI, CH-5232 Villigen, Switzerland
48 DESY, D-15738 Zeuthen, Germany
49 Eidgenössische Technische Hochschule, ETH Zürich, CH-8093 Zürich, Switzerland
§ Supported by the German Bundesministerium für Bildung, Wissenschaft, Forschung und Technologie.
‡ Supported by the Hungarian OTKA fund under contract numbers T019181, F023259 and T037350.
¶ Also supported by the Hungarian OTKA fund under contract number T026178.
♭ Supported also by the Comisión Interministerial de Ciencia y Tecnología.
♯ Also supported by CONICET and Universidad Nacional de La Plata, CC 67, 1900 La Plata, Argentina.
△ Supported by the National Natural Science Foundation of China.

$\sqrt{s}$ (GeV)	188.6	191.6	195.6	199.5	201.7	$202.5 - 205.5$	$205.5 - 207.5$	$207.5 - 209.2$
$\mathcal{L}$ (pb^{-1})	176.8	29.7	83.9	82.8	39.1	77.8	131.4	8.2

Table 1: Centre-of-mass energies and corresponding integrated luminosities, $\mathcal{L}$, considered in this analysis.

	Preselection	Light-Higgs selection	Heavy-Higgs selection
Data	779	345	130
Standard Model	771.8 ± 3.6	347.2 ± 2.0	127.1 ± 1.8
Two-photon interactions	6.4 ± 1.6	–	2.7 ± 1.1
Two-fermion final states	69.9 ± 1.6	2.6 ± 0.3	21.4 ± 0.8
Four-fermion final states	695.5 ± 2.8	344.6 ± 2.0	103.0 ± 1.1

Table 2: Results of the selection of events with hadrons and missing energy. The lower part of the table details the composition of the expected Standard Model sample. The uncertainties reflect the limited background Monte Carlo statistics.

	Efficiency (%)		
m_{h} (GeV)	$\mathrm{Z} \to \mathrm{q\bar{q}}$	$\mathrm{Z} \to \mathrm{e^+e^-}$	$\mathrm{Z} \to \mu^+\mu^-$
60	49.0 ± 1.5	34.2 ± 0.9	22.4 ± 0.8
70	49.8 ± 1.6	38.0 ± 0.8	26.6 ± 0.7
80	49.1 ± 1.8	44.9 ± 0.8	32.7 ± 0.8
90	50.2 ± 1.9	49.9 ± 0.8	31.2 ± 0.8
100	49.4 ± 1.9	40.1 ± 0.8	27.0 ± 0.7
110	47.6 ± 1.7	23.3 ± 0.8	14.8 ± 0.7

Table 3: Selection efficiencies as a function of the mass of the invisibly-decaying Higgs boson. The uncertainties are due to the limited signal Monte Carlo statistics.

	$Z \to e^+e^-$		$Z \to \mu^+\mu^-$	
	Preselection	Selection	Preselection	Selection
Data	147	6	115	9
Standard Model	136.4	9.7	130.2	11.1
$e^+e^- \to e^+e^-(\gamma)$	19.7	0.3	–	–
$e^+e^- \to \mu^+\mu^-(\gamma)$	–	–	12.3	0.8
$e^+e^- \to \tau^+\tau^-(\gamma)$	1.5	–	1.1	–
Two-photon interactions	6.9	–	30.6	–
Four-fermion final states	108.3	9.4	86.2	10.3

Table 4: Results of the selection of events with leptons and missing energy. The lower part of the table details the composition of the expected Standard Model sample. The statistical uncertainties on the background estimation are negligible.

	$Z \to q\bar{q}$		$Z \to e^+e^-$		$Z \to \mu^+\mu^-$	
	Signal	Background	Signal	Background	Signal	Background
Monte Carlo statistics	1.4 %	5.7 %	1.9 %	< 0.1 %	2.5 %	< 0.1 %
Background cross sections	–	3.8 %	–	5.0 %	–	5.0 %
Detector response	2.0 %	4.9 %	2.0 %	2.7 %	2.5 %	4.1 %
Total	2.4 %	8.4 %	2.8 %	5.7 %	3.5 %	6.5 %

Table 5: Relative systematic uncertainties on the signal efficiency and background normalisation for each analysis channel.

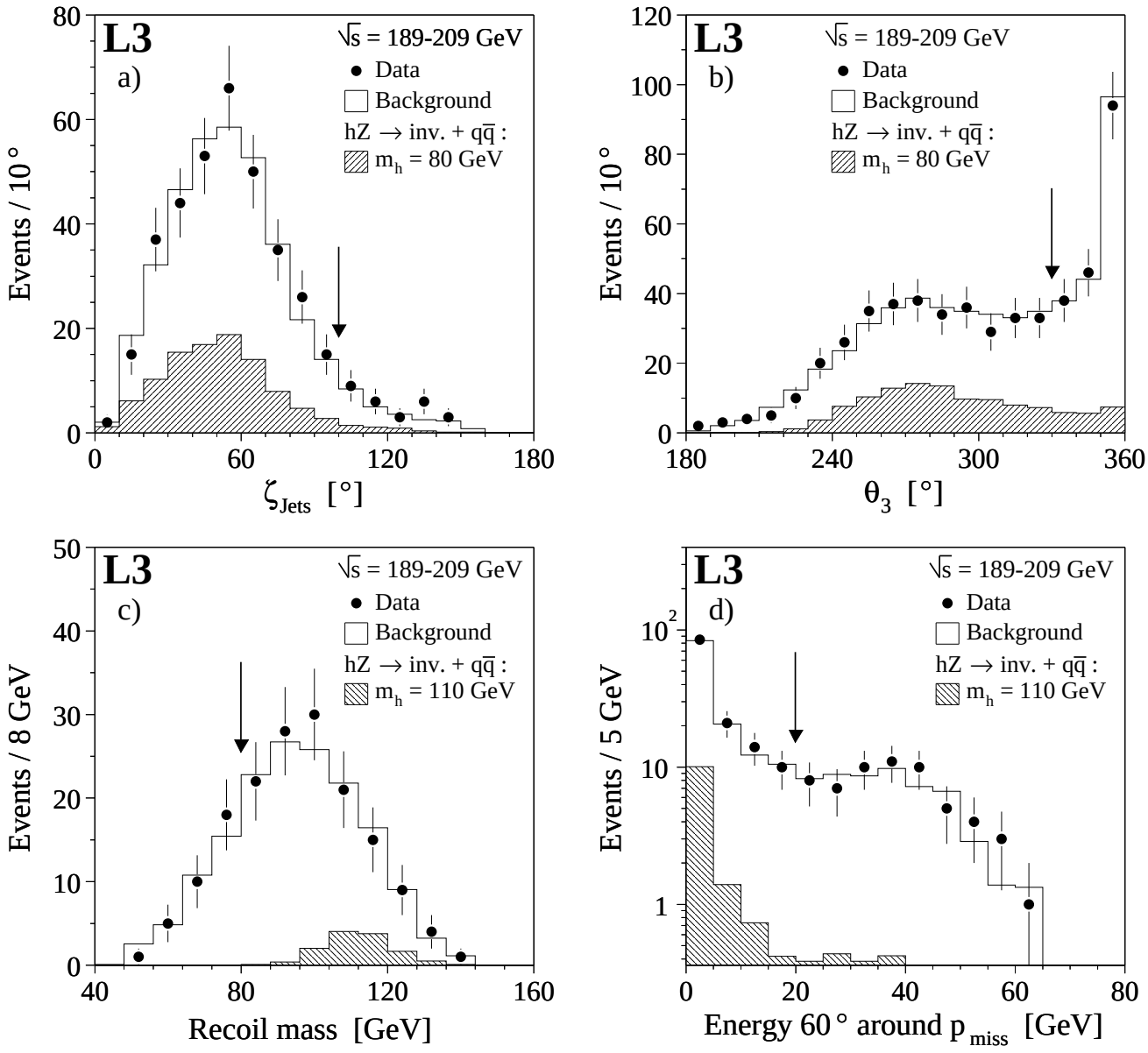

Figure 1: Distributions of variables used in the selection of events with hadrons and missing energy. The dots represent the data, the open area the sum of all background contributions and the hatched histogram the expectation for a signal. The arrows represent the position of the selection criteria.

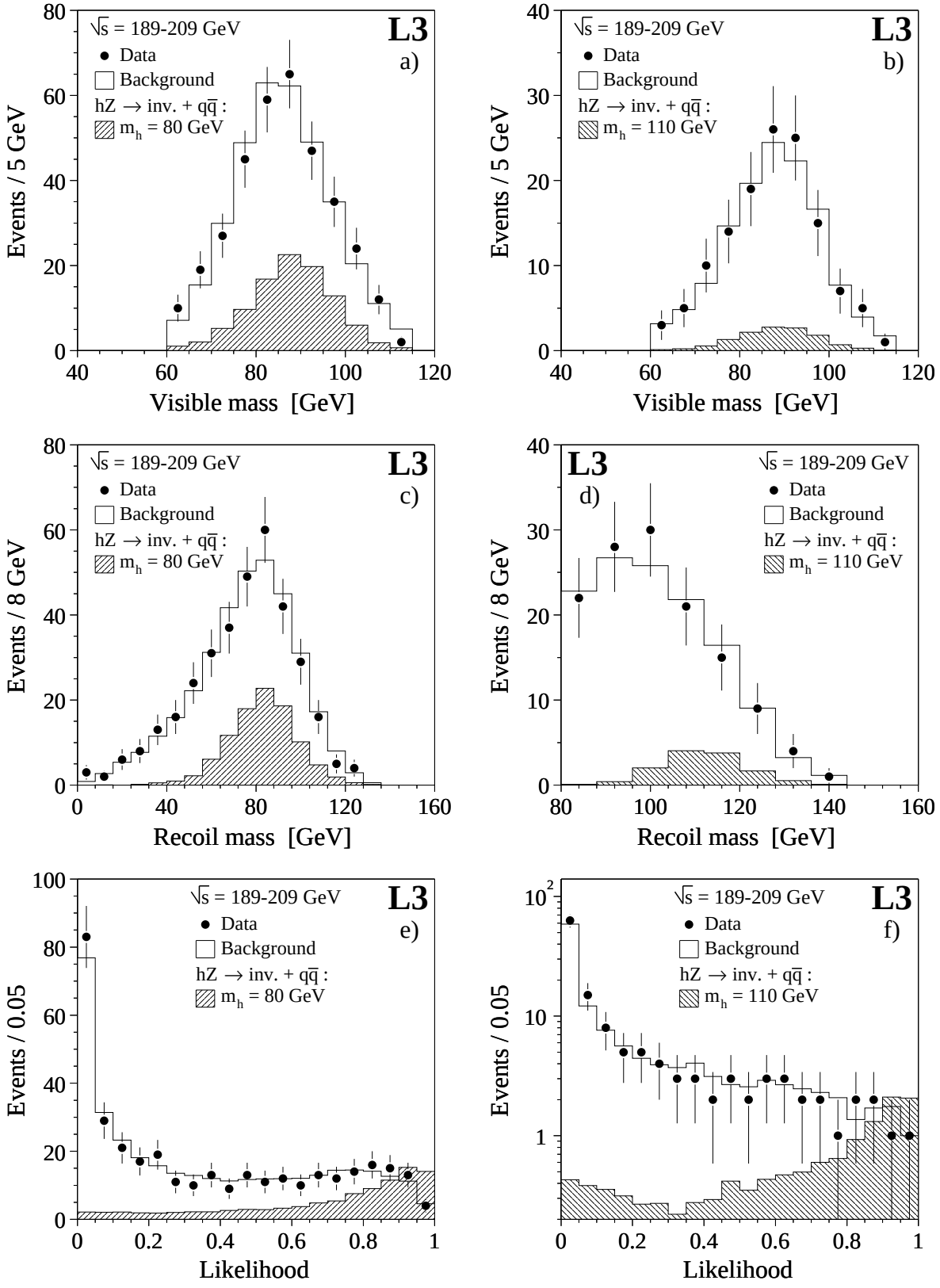

Figure 2: Distributions of the visible and recoil masses for events selected by the light- and heavy-Higgs analyses of events with hadrons and missing energy. The dots represent the data, the open area the sum of all background contributions and the hatched histogram the expectation for a signal. The distributions of the final discriminants used in the analysis are also shown.

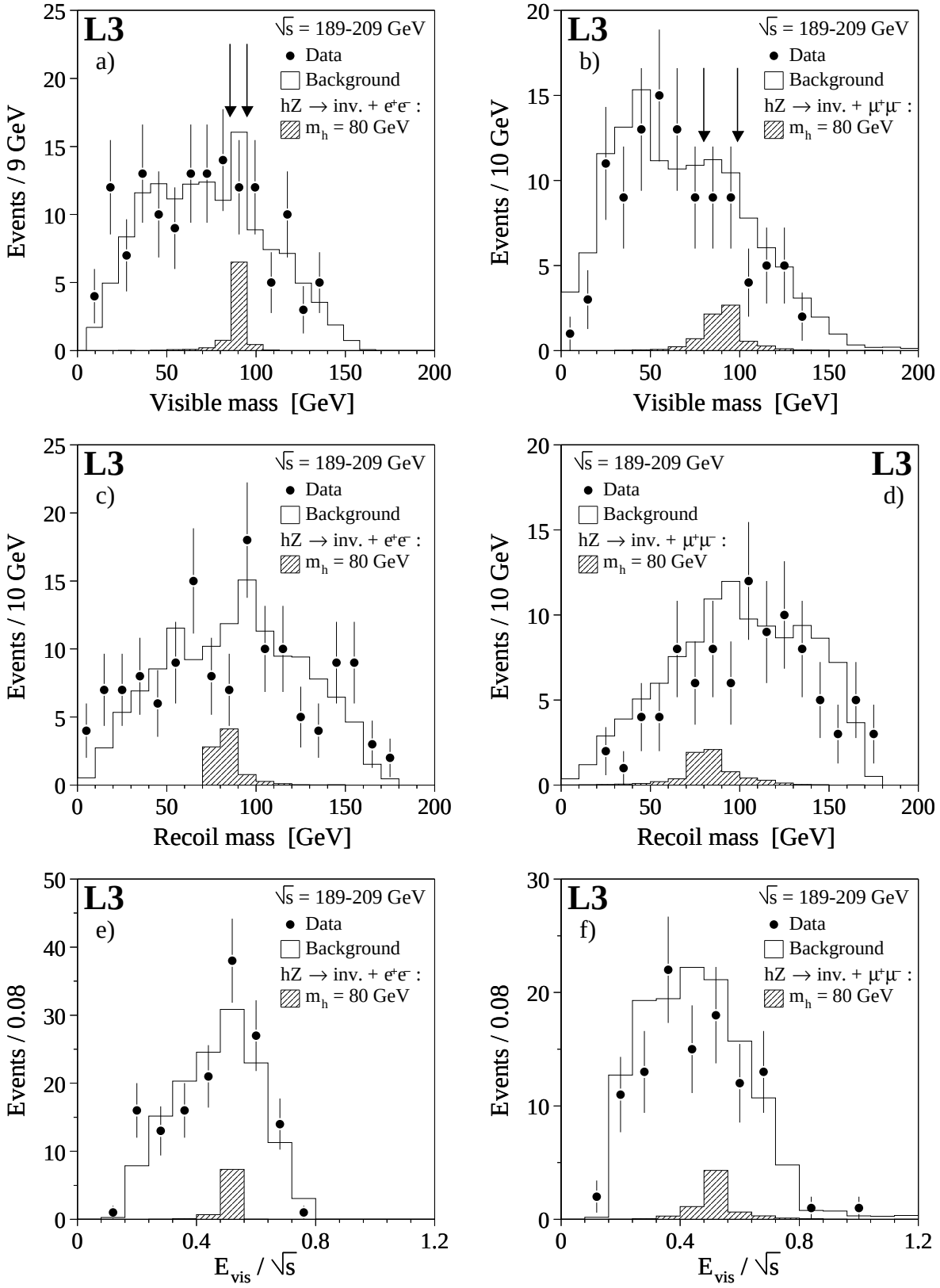

Figure 3: Distributions of the visible and recoil masses and of the visible energy for events with electrons or muons and missing energy. The dots represent the data, the open area the sum of all background contributions and the hatched histogram the expectation for a signal. The selection criteria on the visible masses are illustrated by the arrows.

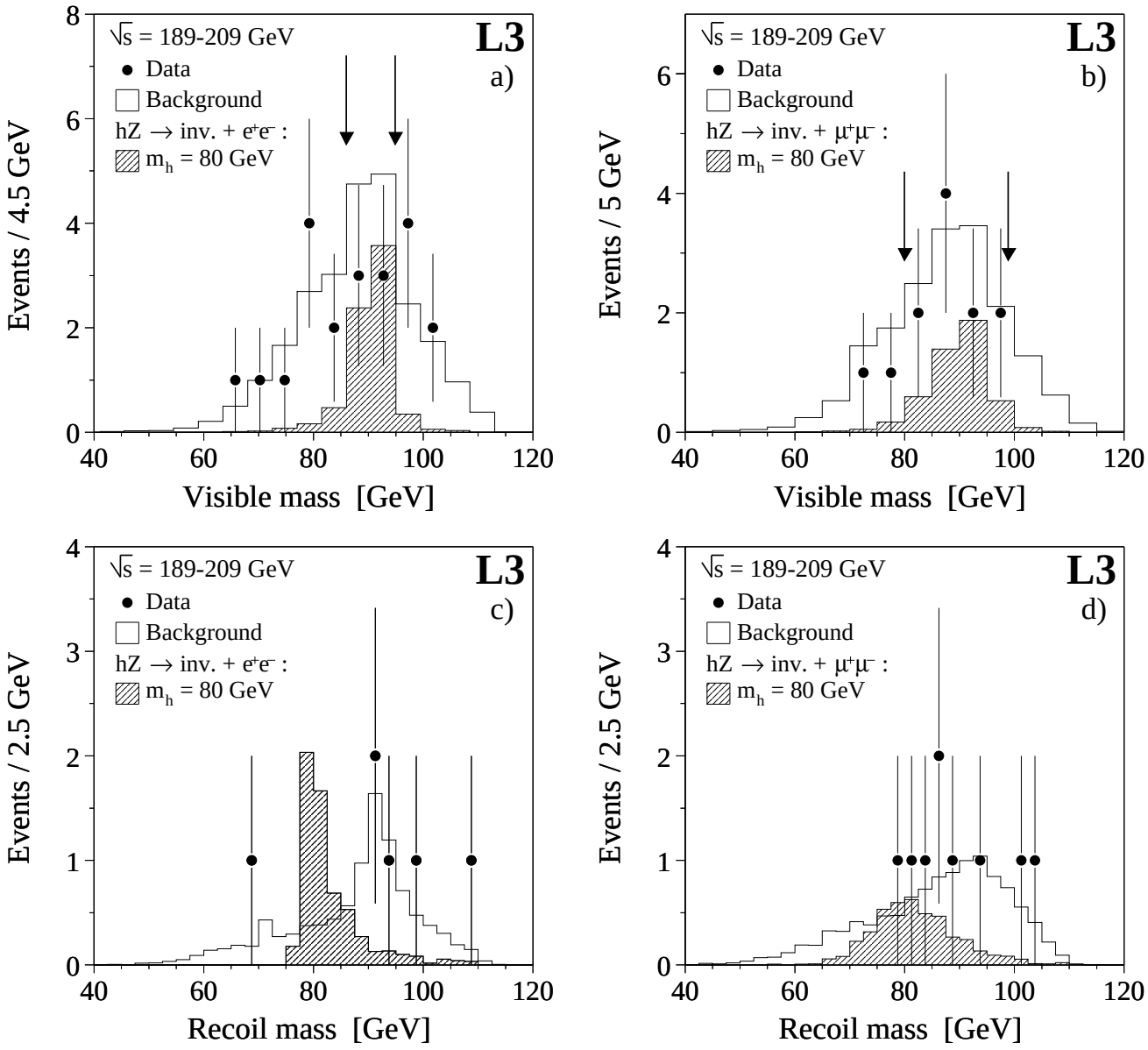

Figure 4: Distributions of the visible mass of events selected by the analysis of final states with a) electrons and missing energy and b) muons and missing energy after. The selection criteria on the visible masses are illustrated by the arrows. Distributions of the recoil mass after the application of all cuts are shown in c) for electrons and d) for muons. The dots represent the data, the open area the sum of all background contributions and the hatched histogram the expectation for a signal.

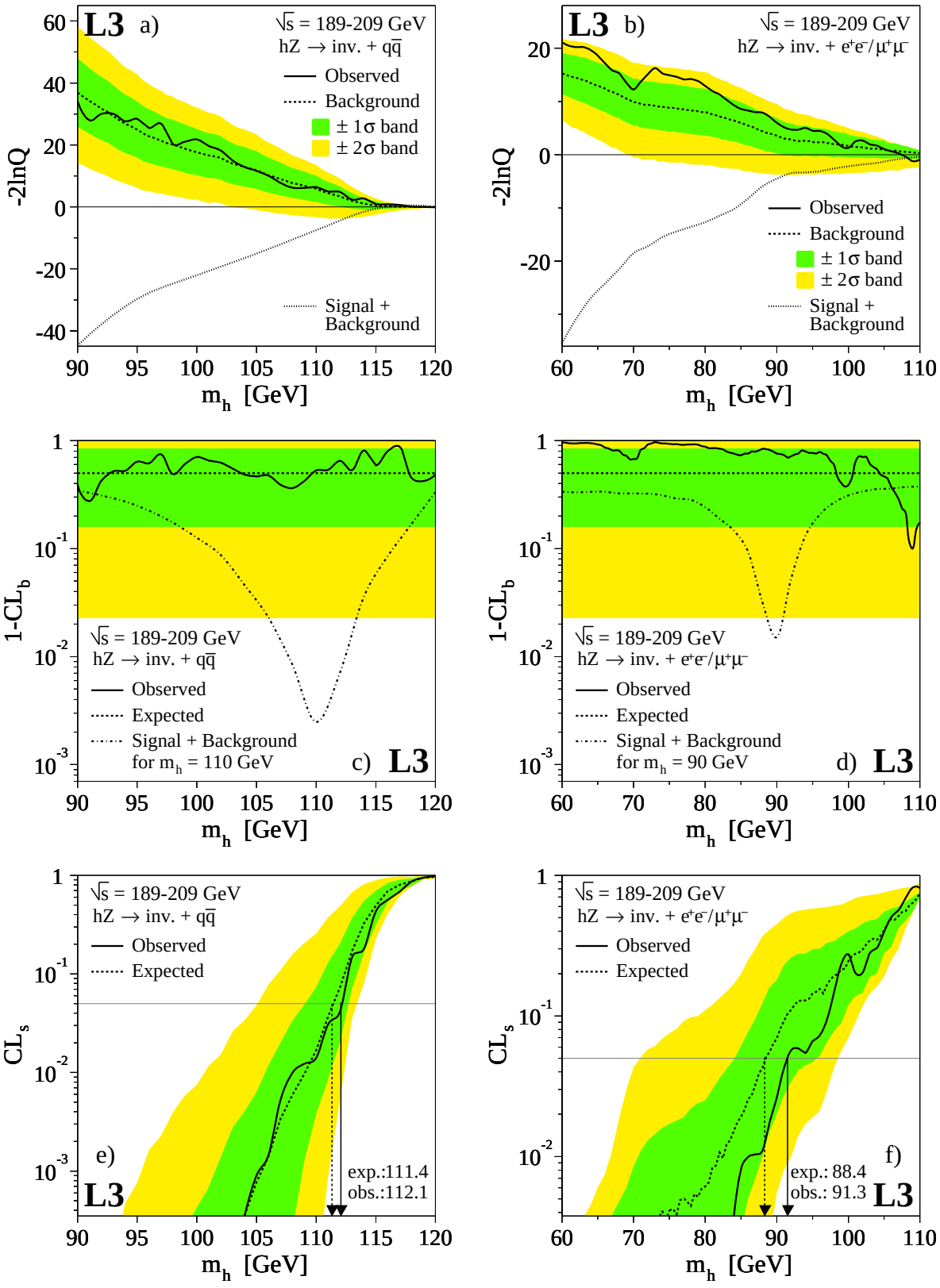

Figure 5: Distributions as a function of m_{h} of the log-likelihood ratio for a) the hadron and b) the lepton analyses; of the $1 - \mathrm{CL_b}$ estimator for c) the hadron and d) the lepton analyses; of the $\mathrm{CL_s}$ estimator for e) the hadron and f) the lepton analyses, together with the expected and observed lower limits on m_{h}.

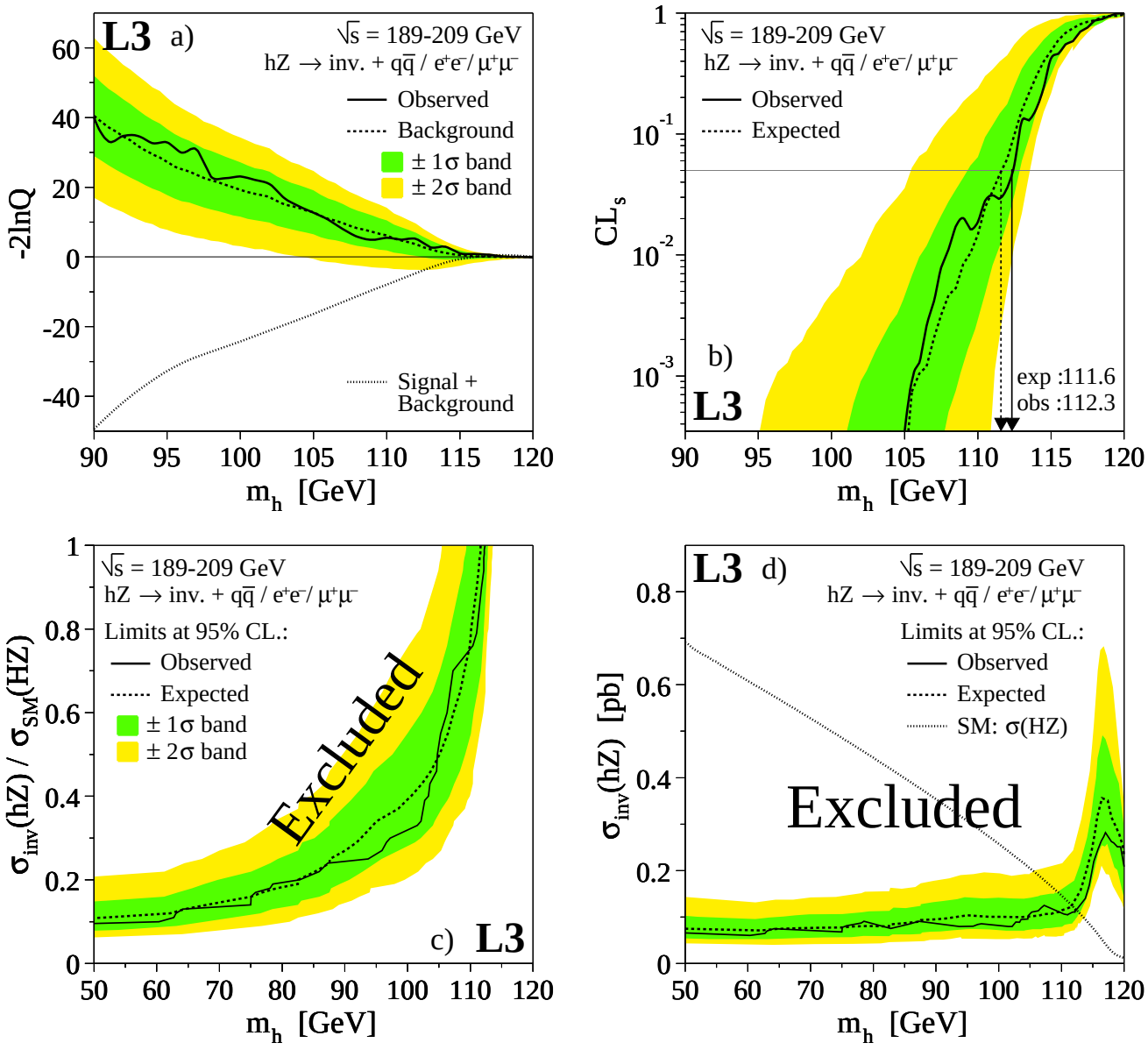

Figure 6: Distributions as a function of m_{h} for the combination of the hadron and lepton analyses of a) the log-likelihood; b) the $\mathrm{CL_s}$ estimator with the expected and observed lower limits on m_{h}; c) upper limits on the ratio of the invisibly-decaying Higgs-boson cross section to the Standard Model one; d) upper limits on the cross section for the production of an invisibly-decaying Higgs boson.